Gap solitons in Bragg gratings with a harmonic superlattice

Kazuyuki Yagasaki[1], Ilya M. Merhasin[2], Boris A. Malomed[2], Thomas Wagenknecht[3] and Alan R. Champneys[3]

[1] *Department of Mechanical and Systems Engineering, Gifu University, Gifu 501-1193, Japan*
[2] *Department of Interdisciplinary Studies, Faculty of Engineering, Tel Aviv University, Tel Aviv 69978, Israel*
[3] *Department of Engineering Mathematics, University of Bristol, Bristol BS8 1TR, UK*

PACS. `42.65.Tg` – Optical solitons; nonlinear guided waves.
PACS. `42.70.Qs` – Photonic bandgap materials.
PACS. `05.45.Yv` – Solitons.

Abstract. – Solitons are studied in a model of a fiber Bragg grating (BG) whose local reflectivity is subjected to periodic modulation. The superlattice opens an infinite number of new bandgaps in the model's spectrum. Averaging and numerical continuation methods show that each gap gives rise to gap solitons (GSs), including asymmetric and double-humped ones, which are not present without the superlattice.Computation of stability eigenvalues and direct simulation reveal the existence of *completely stable* families of fundamental GSs filling the new gaps – also at negative frequencies, where the ordinary GSs are unstable. Moving stable GSs with positive and negative effective mass are found too.

Bragg gratings (BGs) are distributed reflecting structures produced by periodic variation of the refractive index of an optical fiber or waveguide. Devices based on fiber gratings, such as dispersion compensators, sensors and filters, are widely used in optical systems [1]. Gap solitons (GSs) in fiber gratings are supported (in the temporal domain) by the balance between BG-induced linear dispersion, which includes a bandgap in the system's spectrum, and the Kerr nonlinearity of the fiber material. Analytical solutions for BG solitons in the standard model of the fiber grating, based on coupled-mode equations for the right- and left-traveling waves, are well known [3]. Solitons with positive frequency ω are stable, while those with $\omega < 0$ have an instability to perturbations that is characterized by a complex growth rate [4].

Solitons in fiber gratings have been created experimentally, with spatial and temporal widths of the order of a few mm and 50 ps, respectively [5]. Spatial GSs were observed in photorefractive media with an induced photonic lattice [6], and in waveguide arrays [7]. (Indeed, the new families of GSs reported in the present work may be realized in the spatial domain too, in addition to their straightforward implementation as temporal solitons in fiber gratings). Besides their relevance to optical media, GSs were also predicted [8] and created [9] in a Bose-Einstein condensate (BEC) trapped in a periodic potential.

An issue of particular technological importance is the development of methods for the control of BG solitons – in particular, using *apodization* [5, 10, 11], i.e. gradual variation of the grating's reflectivity along the fiber. In an appropriately apodized BG, one can slow down solitons and, eventually, bring them to a halt [11]. Experimentally, it has been demonstrated that apodization helps to couple solitons into the grating [5]. Moreover, technologies are available that allow one to fabricate fiber gratings with *periodic* apodization, thus creating an effective *superlattice* built on top of the BG [12].

An asymptotic analysis of light propagation in such a *superstructure grating* was developed in Ref. [13]. It was shown that the superstructure gives rise to extra gaps in the system's spectrum ("Rowland ghost gaps"). Solitons in the gaps were sought by assuming that the soliton is a slowly varying envelope of the superlattice's Bloch function, which applies to the description of GSs near bandgap edges. Related problems were considered in Refs. [14], which treat BEC models with a doubly periodic optical lattice that opens up an additional narrow "mini-gap", in which stable solitons may be found.

The subject of this Letter is the investigation of GSs in harmonic (sinusoidal) superlattices created on top of the ordinary BG in fibers with Kerr nonlinearity. The analysis of the bandgap structure in this model constitutes, by itself, an interesting extension of the classical spectral theory for the Mathieu equation [15]. We will demonstrate that various families of GSs exist in the superlattice. Most importantly, in each newly opened gap we find a family of fundamental symmetric GSs, which fill the entire gap and are *completely stable*. Remarkably, they are stable not only at positive frequencies ω, but also at $\omega < 0$, where the ordinary GSs are unstable [4].

The superlattice may be implemented via the creation of beatings in the optical interference pattern that burns the grating into the fiber's cladding. A model corresponding to this physical situation may be derived using standard coupled-mode equations for the amplitudes u and v of the right- and left-traveling electromagnetic waves. Inclusion of both Kerr nonlinearity and Bragg reflection terms leads to the following dimensionless equations:

$$\begin{aligned} iu_t + iu_x + [1 - \varepsilon\cos(kx)]\, v + \mu\cos(kx+\delta)\;\; u + \left(|v|^2 + |u|^2/2\right) u &= 0, \\ iv_t - iv_x + [1 - \varepsilon\cos(kx)]\, u + \mu\cos(kx+\delta)\;\; v + \left(|u|^2 + |v|^2/2\right) v &= 0. \end{aligned} \tag{1}$$

Here ε is the amplitude of the periodic modulation of the BG strength, while the nonlinearity coefficient and average reflectivity are normalized, as usual, to be 1. Accordingly, k measures the ratio of the modulation period L to the BG reflection length l (usually, $L \lesssim 1$ cm [12, 13] and $l \sim 1$ mm, while the underlying BG period is ~ 1 μm, whereas the total length of the grating may be up to 1 m). We have included additional terms in Eqs. (1) with amplitude μ and phase shift δ to describe another possible control mechanism for optical pulses in BGs [1,2], namely a periodic *chirp* of the BG, i.e. a local variation of the grating's period.

In this work we focus on the reflectivity superlattice, setting $\mu = 0$; the general situation including the periodic chirp will be considered elsewhere. Thus ε and k are the parameters of the model, which we assume to be positive without loss of generality. According to the above physical considerations, typically ε is small, but k is not. Note that we should only expect a quiescent GS to be stable in this kind of nonuniform BG if the position of the soliton's center is located at a local minimum of the reflectivity [11], i.e. at $x = 2\pi n/k$ for some integer n. Hence we shall restrict our numerical search for GSs to just such a case. Lastly, note that Eqs. (1) conserve two dynamical invariants, the Hamiltonian and norm (usually called *energy* in fiber optics), $E = \int_{-\infty}^{+\infty} \left(|u(x)|^2 + |v(x)|^2\right) dx$.

We shall seek stationary GS in the form $\{u(x,t), v(x,t)\} = \exp(-i\omega t)\,\{U(x), V(x)\}$, sub-

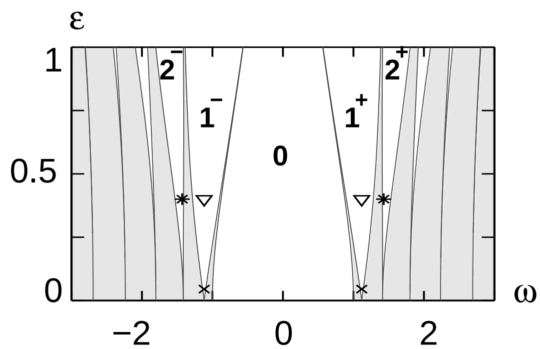

Fig. 1 – The spectrum of Eq. (1) with $k = 1$ in the (ω, ε) plane. Shaded and white areas are, respectively, bands and gaps. Digits label the gaps mentioned in the text. Markers correspond to the solutions plotted in Fig. 2.

stitution of which into Eqs. (1) yields

$$\begin{aligned} \omega U + iU' + [1 - \varepsilon\cos(kx)]\, V + \left(|V|^2 + |U|^2/2\right) U &= 0, \\ \omega V - iV' + [1 - \varepsilon\cos(kx)]\, U + \left(|U|^2 + |V|^2/2\right) V &= 0, \end{aligned} \tag{2}$$

where prime stands for d/dx. First, it is necessary to find bandgaps in the system's spectrum. In the unperturbed problem ($\varepsilon = 0$), the dispersion relation for linear waves with a propagation constant q is $\omega^2 = q^2 + 1$, thus producing the well-known bandgap, $-1 < \omega < 1$. The spectrum for $\varepsilon > 0$ should be found from the linearization of Eqs. (2). As in the Mathieu equation, gaps in these equations emerge due to the parametric resonance caused by the cosine modulation. Straightforward considerations show that new bandgaps open up at points $\omega = \omega_m \equiv \mathrm{sgn}(m)\sqrt{1 + (mk)^2/4}$, with $m = \pm 1, \pm 2, \ldots$ (the extra modulation terms $\sim \mu$ in Eqs. (1) open gaps at the same positions). We will designate these gaps as $\mathbf{m}^{\pm}$. Using perturbation theory, one can find their boundaries for small ε and demonstrate that their widths scale as $\varepsilon^{|m|}$. In particular, gaps $\mathbf{1}^{\pm}$ are found in the region $|\chi| \leq 1$, $\chi \equiv 2\left(\omega - \omega_{\pm 1}\right)/\varepsilon$, to leading-order in ε.

Equations (2) allow the invariant reduction $V = -U^*$, which reduces them to a single equation,

$$\omega U + iU' - [1 - \varepsilon\cos(kx)]\, U^* + (3/2)|U|^2 U = 0 \tag{3}$$

(the reduction with $V = U^*$ leads to an equation with the opposite sign in front of U^*, which can be cast back in the form of Eq. (3) by the substitution $U \equiv i\tilde{U}$; neither reduction is valid for moving solitons, see below). The linearization of Eq. (3) is sufficient for the analysis of the spectrum. Bandgap regions in the (ω, ε)-parameter plane were computed using the software package AUTO with driver HomMap [16]. We detected points at which the linearization of the Poincaré map [17] around the origin ($U = 0$) has eigenvalues ± 1, and then continued such points to identify the bandgap boundaries. The results are displayed in Fig. 1, which shows the first five gaps. In this and subsequent examples, we set $k = 1$, as this value adequately represents the generic situation and is physically meaningful for the application to fiber gratings.

In the central gap, which we designate $\mathbf{0}$, standard calculations using Melnikov's method [17] reveal that the GS solutions, which are known in an exact form for $\varepsilon = 0$ [3], extend to $\varepsilon > 0$. They were continued numerically up to $\varepsilon = 1$, and were found to *completely fill* the central gap. That is, a GS exists for each $\{\omega, \varepsilon\}$-value belonging to the gap. We have also

computed eigenvalues that determine stability of these solutions against small perturbations, and found that only GSs with $\omega > 0$ are stable. That is, the border between stable and unstable GSs in the central gap for $\varepsilon > 0$ is found to remain, up to numerical accuracy, at $\omega = 0$ as it is for $\varepsilon = 0$ [4].

Inside gaps $\mathbf{1}^{\pm}$, one can use the method of averaging [17] to demonstrate the existence of GSs for small ε. To this end, we represent a solution to Eq. (3), $U(x) \equiv a(x) + ib(x)$, as

$$\begin{pmatrix} a \\ b \end{pmatrix} = \sqrt{\varepsilon} \exp\left(\begin{bmatrix} 0 & -(\omega_{\pm 1}+1) \\ \omega_{\pm 1}-1 & 0 \end{bmatrix} x \right) \begin{pmatrix} \Xi/k \\ \Theta/\left(2\left(\omega_{\pm 1}+1\right)\right) \end{pmatrix}. \tag{4}$$

With constant amplitudes Ξ and Θ, we recover a solution to the linearized equation (3) with $\varepsilon = 0$ and $\omega = \omega_{\pm}$. The averaging method supposes that Ξ and Θ are functions of a slow coordinate, $z \equiv x/\left[2k(\omega_{\pm 1}+1)\right]$, which leads to equations

$$\frac{d}{dz} \begin{pmatrix} \Xi \\ \Theta \end{pmatrix} = \begin{pmatrix} \alpha(1-\chi)\Theta - \beta\left(\Xi^2+\Theta^2\right)\Theta \\ \alpha(1+\chi)\Xi + \beta\left(\Xi^2+\Theta^2\right)\Xi \end{pmatrix}, \tag{5}$$

where $\alpha \equiv \varepsilon\left[k^2 + 4(\omega_{\pm 1}+1)^2\right]$, and $\beta \equiv 3\varepsilon[3k^4 + 8(\omega_{\pm 1}+1)^2 k^2 + 48(\omega_{\pm 1}+1)^4]/[8k(\omega_{\pm 1}+1)]^2$. These equations conserve their Hamiltonian, $H = \alpha\left[(1+\chi)\Xi^2 - (1-\chi)\Theta^2\right] + (\beta/2)\left(\Xi^2+\Theta^2\right)^2$. As gaps $\mathbf{1}^{\pm}$ exist for $|\chi| < 1$, the coefficients $1 \mp \chi$ in Eqs. (5) and in H are positive. Therefore, the origin $(\Xi, \Theta) = (0, 0)$ is a saddle in Eqs. (5), and a pair of homoclinic orbits to this saddle can be found in the exact form

$$(\tilde{\Xi}_{\pm}(t), \tilde{\Theta}_{\pm}(t)) = \left(\pm 2\sqrt{\frac{\alpha}{3\beta}} \sin\theta \sin\frac{\theta}{2} \frac{\sinh(\alpha t \sin\theta)}{\cosh(2\alpha t \sin\theta) + \cos\theta}, \right. \tag{6}$$

$$\left. \mp 2\sqrt{\frac{\alpha}{3\beta}} \sin\theta \cos\frac{\theta}{2} \frac{\cosh(\alpha t \sin\theta)}{\cosh(2\alpha t \sin\theta) + \cos\theta} \right), \tag{7}$$

with $\chi \equiv \cos\theta$. On application of the transformation (4), these orbits correspond to solitons in the full system (3). In particular, there are solutions with $a(x) = \mathrm{Re}\, U(x)$ odd and $b(x) = \mathrm{Im}\, U(x)$ even. Thus, GSs exist in the entire gaps $\mathbf{1}^{\pm}$ for sufficiently small ε.

A similar analysis can be performed for higher bandgaps, $\mathbf{2}^{\pm}$, $\mathbf{3}^{\pm}$, etc., using a higher-order averaging method [18]. The respective analytical computations show that each averaged system again generates solitons. They have either even real and odd imaginary parts or vice versa, depending on whether the gap's number m is odd or even.

We employed the AUTO driver HomMap [16] to continue numerical soliton solutions of the full system (3), varying ω and ε . In so doing, a multitude of symmetric and *asymmetric* families of GS solutions, including higher-order ones (bound states) were found in each new gap. Here, we display numerical results for fundamental solitons, as their bound states are likely to be unstable. It was found that, as predicted above, each gap $\mathbf{1}^{\pm}$, $\mathbf{2}^{\pm}$, etc. is completely filled with a single family of symmetric GSs. The families in gaps $\mathbf{1}^{\pm}$ are represented by solitons displayed in Figs. 2(a$^{\pm}$) and (b$^{\pm}$), for small and larger ε, respectively, while Figs. 2(c$^{\pm}$) displays the fundamental GSs in gaps $\mathbf{2}^{\pm}$. Note that stable fundamental solitons may feature a *double-humped structure* in terms of $|U(x)|$ at relatively large ε, which is the case for the soliton in Fig. 2(b^{+}), see Fig. 3(b) below (however, the $|U(x)|$ profile of the GS displayed, for the same ε but opposite ω, in panel 2(b^{-}), remains single-humped, see Fig. 3(a)). The homoclinic orbits of averaged system (5), also shown in a) and c), provide a good match to the envelopes of the numerical solutions.

Recall that the ordinary GSs in gap $\mathbf{0}$ with $\varepsilon = 0$ cannot be asymmetric, and they do not form bound states either [2]. To explain where the asymmetric and higher-order GSs for

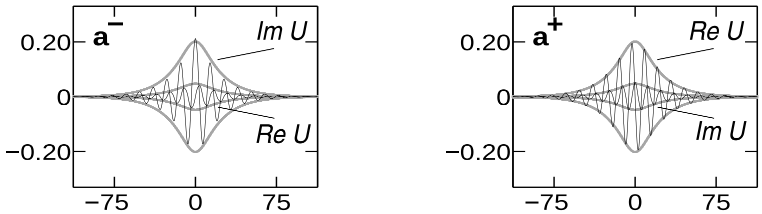

a) $\omega = \mp 1.118$, $\varepsilon = 0.045$, $k = 1$ (points $\times$ in Fig. 1)

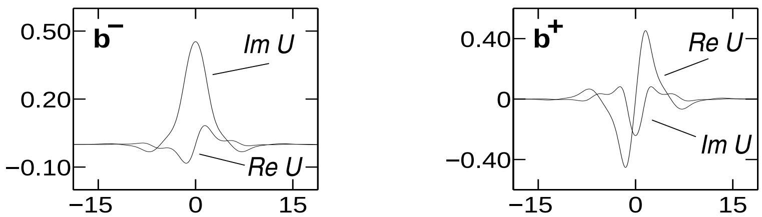

b) $\omega = \mp 1.118$, $\varepsilon = 0.4$, $k = 1$ (points ∇ in Fig. 1)

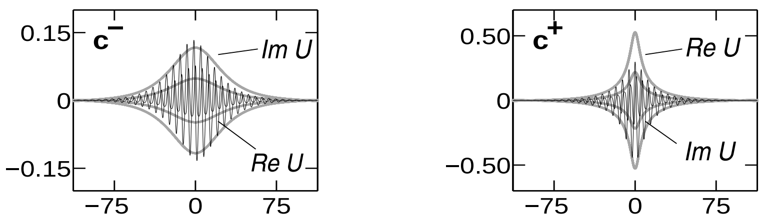

c) $\omega = \mp 1.42$, $\varepsilon = 0.4$, $k = 1$ (points $\ast$ in Fig. 1)

Fig. 2 – Stable fundamental soliton solutions of Eq. (3) in gaps $\mathbf{1}^{\pm}$ and $\mathbf{2}^{\pm}$. Gray lines in rows a) and c) show solutions of averaged equations (5), and their counterparts for gaps $\mathbf{2}^{\pm}$.

$\varepsilon > 0$ come from, we note that the new symmetric fundamental GSs, found above in gaps $\mathbf{1}^{\pm}$, correspond to transversal intersections of stable and unstable manifolds in the Poincaré map associated with Eq. (3). Such intersections naturally occur in pairs, one representing a symmetric soliton and the other one its asymmetric counterpart. Moreover, the transversality of the intersection implies the presence of a Smale horseshoe [17], which, in turn, ensures the existence of infinitely many higher-order GSs, that may be realized as bound states of symmetric or asymmetric fundamental solitons.

Stability of the GSs was tested by direct simulations of Eqs. (1), and verified through computation of the eigenvalues of the equations linearized around a GS, which govern the growth rate of small perturbations. Using this approach, it was found that the *entire* families of the symmetric fundamental solitons that fill the gaps $\mathbf{1}^{+}$ and $\mathbf{1}^{-}$ are stable. The significance of this result is that we can have *stable GSs* with $\omega < 0$, something, that is not possible in the ordinary BG model without the periodic modulation terms. This finding is illustrated in Fig. 3(a), taking as an example the soliton with $\omega = -1.118$ depicted in Fig. 2(b^{-}).

Regarding asymmetric solitons in gaps $\mathbf{m}^{\pm}$ with $m \geq 1$, it was found that some of them are stable and some are not, the unstable ones being completely destroyed by growing perturbations (not shown here).

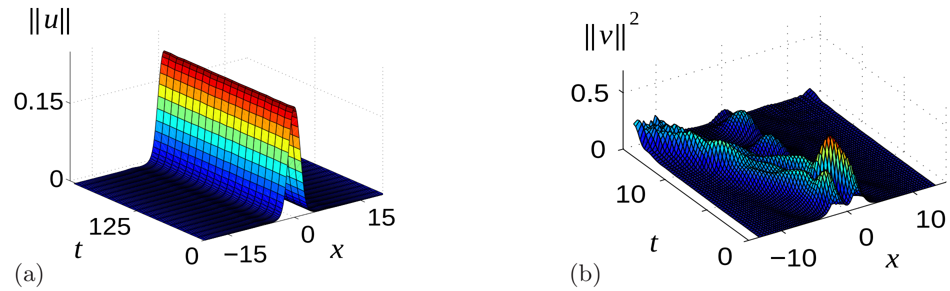

Fig. 3 – Soliton dynamics in gaps $\mathbf{1}^{\mp}$. (a) Evolution of a perturbed symmetric soliton shown in Fig. 2(b$^-$) ($\varepsilon = 0.4$, $\omega = -1.118$; for these ε and ω, an asymmetric soliton exists too, but it is unstable). (b) Splitting of the stable double-humped soliton shown in Fig. 2(b$^+$) into moving and quiescent ones, after it was suddenly multiplied by $\exp(ipx)$, with $p = 1$.

An important issue for practical application is the possibility of finding moving GSs. (In experiments on ordinary fiber gratings, only moving solitons have so far been observed [5]). In the presence of the superlattice, soliton mobility is a nontrivial problem, because the GS has to move in a periodically nonuniform medium. (Recall, though, that solitons belonging to gaps $\mathbf{m}^{\pm}$ with $m \geq 1$ do not exist at all without the superlattice). We have used numerical simulation to test for mobility of the stable GSs we have so-far found. Specifically, a quiescent stable soliton was multiplied by $\exp(ipx)$, with $p > 0$, which implies a sudden application of a "shove" to the soliton, giving it momentum $P = i\int_{-\infty}^{+\infty}(uu_x^* + vv_x^*)\,dx + \text{c.c.} \equiv 2pE$, where E is the soliton's energy defined above. It was observed that GSs belonging to central gap $\mathbf{0}$ are readily set in stable motion by the shove. This accords with the situation for $\varepsilon = 0$, where exact solutions for moving GSs exist with any velocity c from $-1 < c < +1$ [3]. In our simulations, we found that no soliton in any gap could be made to move with velocity exceeding 1 (a very strong shove does not make the GS "superluminal", but simply destroys it).

For the stable GS belonging to gap $\mathbf{1}^+$, it was found that the application of the shove caused the soliton to split into a quiescent part and a moving part; see Fig. 3(b). A remarkable observation from these results is that the moving soliton (which retains $\simeq 2/3$ of the initial energy) has a negative average velocity, $c \approx -0.9$, hence its effective mass $M \sim P/c$ is *negative* too. (Simulations of the moving GSs belonging to gap $\mathbf{0}$ have positive mass, as is the case for $\varepsilon = 0$ [11]). We remark that the mass of a GS may be negative too in one- and two-dimensional models of BEC in an ordinary optical lattice, and that this gives rise to nontrivial effects such as stable confinement of solitons in an *anti-trapping* external potential [19]. Finally, the shove applied to a stable GS belonging to gap $\mathbf{1}^-$ was found to split into three solitons, one remaining quiescent while the other two move off in opposite directions (not shown here). Detailed results for moving solitons will be reported elsewhere.

In conclusion, we have investigated a model for a Bragg grating optical fibre with a superlattice written on top. First, we identified a system of new bandgaps in the fiber's spectrum, using an extension of the bandgap theory for the Mathieu equation. Combining averaging methods and numerical continuation, we have found that each new gap is completely filled with fundamental symmetric solitons, which at some parameter values may have a double-humped shape. In addition, new types of gap solitons (GSs) were found that do not exist without the superlattice, such as asymmetric GSs and bound states of fundamental GSs. An

important finding is that the entire families of fundamental GSs in the new bandgaps are stable, including negative frequencies, where ordinary GSs are unstable. Stable moving solitons were found too, including ones with a negative mass. Finally, it is pertinent to point out that creation of the newly predicted GSs ought to be perfectly feasible using presently available experimental techniques. In particular, in a weak superlattice, with say, $\varepsilon \simeq 0.1$, an estimate shows that the solitons in the new bandgaps $\mathbf{1}^{\pm}$ can be observed if the fiber grating, on top of which the superlattice is to be imposed, is of length $\simeq 10$ cm.

* * *

K.Y. acknowledges support from the Japan Society for the Promotion of Science for his stay at the University of Bristol. I.M.M. and B.A.M. appreciate support from the Israel Science Foundation, through the Center-of-Excellence grant No. 8006/03, and from EPSRC, UK. They thank the Department of Engineering Mathematics at the University of Bristol for its hospitality. T.W. acknowledges EPSRC support.

REFERENCES

[1] KASHYAP R., *Fiber Bragg gratings* (Academic Press, San Diego) 1999.
[2] DE STERKE C. M. and SIPE J. E., *Progr. Opt.*, **33** (1994)203.
[3] ACEVES A. B. and WABNITZ S., *Phys. Lett. A*, (1989) **141** 37; CHRISTODOULIDES D. N. and JOSEPH R. I., *Phys. Rev. Lett.*, **62** (1989) 1746.
[4] MALOMED B. A. and TASGAL R. S., *Phys. Rev. E*, **49** (1994) 5787; BARASHENKOV I. V., PELINOVSKY D. E. and ZEMLYANAYA E. V., *Phys. Rev. Lett.*, **80** (1998) 5117.
[5] EGGLETON B. J. *et al.*,, *Phys. Rev. Lett.*, **76**, 1627 (1996); EGGLETON B. J., DE STERKE C. M. and SLUSHER R. E., *J. Opt. Soc. Am. B*, **16** (1999) 587.
[6] MANELA, O. *et al.*,, *Opt. Lett.*, **29** (2004) 2049; BARTAL G. *et al.*,, *Phys. Rev. Lett.*, **95** (2005) 053904.
[7] LAHINI Y., MANDELIK D. and SILBERBERG Y., *Opt. Exp.*, **13** (2005) 1762.
[8] BAIZAKOV B. B., KONOTOP V. V. and SALERNO M., *J. Phys. B*, **35** (2002) 5115; OSTROVSKAYA E. A. and KIVSHAR Y. S.,, *Phys. Rev. Lett.*, **90** (2003) 160407.
[9] EIERMANN, B. *et al.*,, *Phys. Rev. Lett.*, **92** (2004) 230401.
[10] SLUSHER R. E. *et al.*,, *Opt. Exp.*, **3** (1998) 465.
[11] MAK W. C. K., MALOMED B. A. and CHU P. L., *J. Mod. Opt.*, **51** (2004) 2141; JANNER D. *et al.*,, *Phys. Rev. E*, **72** (2005) 056605.
[12] RUSSELL P. ST. J., *J. Appl. Phys.*, **59** (1986) 3344.
[13] BRODERICK N. G. R. and DE STERKE C. M., *Phys. Rev. E*, **55** (1997) 3634.
[14] LOUIS P. J. Y., OSTROVSKAYA E. A. and KIVSHAR Y. S., *Phys. Rev. A*, **71** (2005) 023612; PORTER M. A. and KEVREKIDIS P. G., *SIAM J. Appl. Dyn. Syst.*, **4** (2005) 783; PORTER M. A. *et al.*,, *Phys. Lett. A*,, in press (article PLA15176).
[15] SMITH P. and JORDAN D. W., *Nonlinear Ordinary Differential Equations: An Introduction to Dynamical Systems* 3rd. ed. (Oxford University Press, Oxford) 1999.
[16] DOEDEL E. J. *et al.*,, AUTO97 *Continuation and bifurcation software for ordinary differential equations* 1997, available at `http://cmvl.cs.concordia.ca/auto/`; YAGASAKI K., *Int. J. Bif. Chaos*, **8** (1998) 1617.
[17] GUCKENHEIMER J. and HOLMES P., *Nonlinear Oscillations, Dynamical Systems, and Bifurcations of Vector Fields* (Springer, New York) 1983.
[18] YAGASAKI K., *Nonlin. Dyn.*, **18** (1999) 129; YAGASAKI K. and ICHIKAWA T., *Int. J. Bif. Chaos*, **9** (1999) 519.
[19] SAKAGUCHI H. and MALOMED B. A., *J. Phys. B*, **37** (2004) 1443; 2225.